Hindawi
Journal of Chemistry
Volume 2022, Article ID 1111817, 10 pages
https://doi.org/10.1155/2022/1111817

Research Article

Chemical Constituents of the Bark of *Zanthoxylum gilletii* (Rutaceae) and Their *In Vitro* Antiplasmodial and Molecular Docking Studies

Liliane Clotilde Dzouemo,[1] **Gervais Mouthé Happi**,[2] **Sikiru Akinyeye Ahmed**,[3] **Willifred Dongmo Tekapi Tsopgni**,[1] **Michael Nde Akuma**,[2] **Shina Salau**,[3] **Emmanuel Ngeufa Happi**,[1] **and Jean Duplex Wansi**[1]

[1]*Department of Chemistry, Faculty of Sciences, University of Douala, Douala, P.O. Box 24157, Cameroon*
[2]*Department of Chemistry, Higher Teacher Training College, The University of Bamenda, Bambili, P.O. Box 39, Cameroon*
[3]*Department of Chemistry and Industrial Chemistry, Kwara State University, Malete 23431, Ilorin, P.M.B 1530, Nigeria*

Correspondence should be addressed to Gervais Mouthé Happi; gervais20022003@yahoo.fr and Jean Duplex Wansi; jdwansi@yahoo.fr

Received 3 August 2022; Revised 5 October 2022; Accepted 14 November 2022; Published 22 November 2022

Academic Editor: Vinod Kumar Tiwari

The phytochemical investigations of the methanol extract of *Zanthoxylum gilletii* bark led to the isolation of thirteen compounds identified as two alkaloids including one acridone 5-hydroxynoracronycine (**1**) and one benzo [*c*] phenanthridine decarine (**2**), three lignans *trans*- and *cis*-fagaramide (**3** and **4**) and sesamin (**5**), two coumarins scoparone (**6**) and scopoletin (**7**), three pentacyclic triterpenoids fridelin (**8**), lupeol (**9**) and erythrodiol-3-O-palmitate (**10**), one phenolic compound vanillic acid (**11**) as well as two common steroids stigmasterol (**12**), and its derivative stigmasterol-3-O-*β*-D-glucopyranoside (**13**). The structures of all the isolated compounds were elucidated by means of their spectroscopic and spectrometric data (1D, 2D-NMR, MS) as well as the comparison of these data with those reported in the literature. Except for compounds **9** and **11**–**13**, all the other isolated compounds are reported for the first time from *Z. gilletii* but have been already obtained from other *Zanthoxylum* species and in the Rutaceae family. Compounds **1**, **3**–**5**, and **9** were tested *in vitro* for their antiplasmodial potencies against *Plasmodium falciparum* 3D7, and the results revealed that all the tested compounds displayed an inhibition between 51.89% and 54.69% while only the mixture of **3** + **4** gave an IC_{50} lower than 10 000 nM (IC_{50} = 1333 nM). Furthermore, all the compounds have been evaluated *in silico* for their ability to inhibit the *Plasmodium falciparum* dihydroorotate dehydrogenase 5TBO. Sesamin (**5**) showed the greatest affinity to the antiplasmodium receptor than artemether® and chloroquine®. Further recorded data from their ADMET study, as well as their chemotaxonomy, are also discussed herein. The present study provides further information to enrich the chemistry of *Z. gilletii* and its qualification as an important source for good candidates in new antiplasmodial drug development.

1. Introduction

Malaria is a parasitic disease with a great incidence in the public health sector in many countries in tropical areas of the world [1]. A recent report by the World Health Organization (WHO) indicated that 228 million cases of malaria have been recorded in the world with 405 thousand deaths including almost 94% occurring in Africa. More specifically, fifteen African countries accounted for 80% of global malaria deaths while 2,974,819 confirmed cases and an estimation of 14,841 deaths have been reported in Cameroon during the year 2020 [2, 3]. The disease is caused by the parasite *Plasmodium* transmitted through the bites of the mosquitoes *Anopheles* [1, 4]. It is well reported that medicinal plants represent an important source of bioactive compounds that can be considered as good candidates in the development of

new potent drugs. For instance, the well-known antimalarial drug artemisinin was initially obtained from the plant *Artemisia annua* while quinine was isolated from *Cinchona officinalis* [5]. Unfortunately, the observed rise of resistance of *P. falciparum* to the available antimalarial drugs keeps actual the search for new affordable and potent compounds that can be developed as drugs. *Zanthoxylum gilletii* (Rutaceae) also called *Z. macrophylla*, *Fagara tessmanii*, or *F. macrophylla* is a tree encountered in the tropical rainforest that can reach 10 to 35 m high [6, 7]. The plant is one of the 2000 species that constituted the genus *Zanthoxylum* and its synonyms in the genus *Fagara* which are widely used in African folk medicine for the treatment of several diseases [8]. The stem bark of *Z. gilletii* is used in Cameroon and Madagascar for the treatment of microbial infection, cancer, inflammation, hypertension, and related disorders while its bark is used in Kenya and Ivory Coast against malaria [8]. The use of *Z. gilletii* in the management of malaria has been further supported by the good antimalarial activity of its ethanolic extract against a panel of *Plasmodium falciparum* strains with an IC_{50} value of 5 μg/mL [9]. As a continuity of our program in searching for antiplasmodial agents from Cameroonian medicinal plants [1, 10], we carried out phytochemical investigations of the bark of *Z. gilletii*. In addition, the *in silico* study of the isolated compounds as potential inhibitors of the 5TBO receptor (*Plasmodium falciparum* dihydroorotate dehydrogenase) as well as their ADMET evaluation and chemotaxonomy have been done, and the results are herein discussed. This study provides additional compounds to enrich the chemistry of *Z. gilletii*, its chemotaxonomic classification in the family Rutaceae as well as it further supports its use in folk medicine by the local population for the management of malaria and related symptoms.

2. Materials and Methods

2.1. General Instrumentation. EI-MS were recorded on a Finnigan MAT 95 spectrometer (70 eV) (Thermo Fisher Scientific, Darmstadt, Germany) with perfluorokerosene as a reference substance for EI-HR-MS. The spectrometer operated in positive and negative modes (*m/z*: 50–1500, with a scan rate of 1.00 Hz) with automatic gain control to provide high-accuracy mass measurements within 1 ppm deviation using Na formate as a calibrant. The following parameters were used for experiments: spray voltage of 4.5 kV and the capillary temperature of 200°C. Nitrogen was used as sheath gas (4 l/min). The ^{1}H- and ^{13}C-NMR spectra were recorded at 500 MHz and 125 MHz, respectively, on Bruker AMX 500 NMR spectrometers (Bruker, Rheinstetten, Germany). Chemical shifts are reported in δ (ppm) using TMS as an internal standard, and coupling constants (J) were measured in Hz. Column chromatography was carried out on silica gel (70–230 mesh (Merck, Darmstadt, Germany). Thin-layer chromatography (TLC) was performed on Merck precoated silica gel 60 F_{254} aluminium foil (Merck, Darmstadt, Germany), and spots were detected using ceric sulphate spray reagent. All reagents used were of analytical grade.

2.2. Plant Material. The stem bark of *Zanthoxylum gilletii* (De Wild.) P. G. Waterman was harvested at Bana-Tentcheu (GPS coordinates: Latitude 5°07′57″N, Longitude 10°17′41″E, Elevation: 1412 m), West region, Cameroon, in April 2021. Some leave and bark samples have been used for the identification of the plant by Mr. Victor Nana in comparison with the plant material available in the National Herbarium of Cameroon database where a specimen was registered under the voucher number 38960 HNC.

2.3. Extraction and Isolation. The yellowish bark of *Z. gilletii* (3.8 kg) has been dried and grounded to obtain a powder that was twice extracted with methanol at room temperature for 48 h, each, to afford 148.3 g of crude extract after removing solvent. After keeping a small amount for biological tests and further chemical analyses, 130 g of crude extract was dissolved in water and successively partitioned with ethyl acetate (EtOAc) and *n*-butanol to give two main fractions A (78.4 g) and B (46.8 g). The ethyl acetate soluble fraction A has been further chromatographed over a silica gel column (230–400 mesh, 5.0 × 75.0 cm) eluting with increasing polarity of ethyl acetate in *n*-hexane (*n*-Hex) followed by the gradient of methanol in ethyl acetate. A total of 563 subfractions (ca. 200 mL each) were collected and combined into 6 series A1–A6 based on their TLC profiles.

Further purification of series A1 (14.2 g, *n*-Hex/EtOAc 9 : 1) using column chromatography led to the precipitation of four compounds at four different successive polarities including compound **8** (3.3 mg) at *n*-Hex/EtOAc 39 : 1, compound **12** (20.6 mg) at *n*-Hex/EtOAc 19 : 1, compound **10** (4.2 mg) at *n*-Hex/EtOAc 37 : 3, and compound **9** (47.8 mg) at *n*-Hex/EtOAc 9 : 1.

Likewise, the second series A2 (12.7 g, *n*-Hex/EtOAc 8 : 2) was also subjected to column chromatography over silica gel eluting with a gradient of EtOAc in *n*-Hex from 9 : 1 to 3 : 1 and allowed the collection of 132 subfractions (100 mL each) and the filtration of four distinct pure compounds **1** (19.3 mg), **2** (3.6 mg), **5** (32.4 mg), and **11** (2.4 mg) from the subfractions obtained at the polarity between *n*-Hex/EtOAc 17 : 3 and *n*-Hex/EtOAc 8 : 2.

A third series A3 (8.2 g, *n*-Hex/EtOAc 7 : 3) has been further purified using the same chromatographic technique to afford 115 subfractions from which the unseparated mixture of compounds **3** and **4** (8.3 mg) was obtained at *n*-Hex/EtOAc 3 : 1, and compound **6** (3.2 mg) was obtained after column chromatography using Sephadex LH_{20} of the subfractions 64–86 (2.1 g, *n*-Hex/EtOAc 7 : 3) eluting isocratically with methanol.

Finally, the series A4 (10.3 g, *n*-Hex/EtOAc 1 : 1) and A5 (11.4 g, EtOAc) were mixed and chromatographed using a gradient of methanol in dichloromethane to obtain compounds **7** (2.8 mg) and **13** (28.7 mg), while the last series A6 (18.1 g, AE/MeOH 5%) has been mixed to the *n*-BuOH soluble main fraction B and subjected to column chromatography using the increasing polarity of methanol in EtOAc to afford compound **13** (3.8 mg), and some precipitates are insoluble in the organic solvent.

2.4. Plasmodium falciparum Culture and Growth Inhibition Assay. *Plasmodium falciparum* 3D7 (chloroquine-sensitive) strain was obtained from the Biodefense and Emerging Infections (BEI) Research Resources (Manassas, VA) and maintained using a modified Trager and Jensen method. The biological assay has been done following a modified method of Yemback et al. [11]. Briefly, parasites were cultured in fresh O^+ human red blood cells at 3% (v/v) hematocrit in RPMI 1640 culture media containing GlutaMAX and $NaHCO_3$ (Gibco, UK) and supplemented with 25 mM HEPES (Gibco, UK), 1X hypoxanthine (Gibco, USA), 20 μg/mL gentamicin (Gibco, China), and 0.5% Albumax II (Gibco, USA). When needed, parasites were synchronized at the ring stage by sorbitol treatment and cultured through one cycle before treatment.

Stock solutions (10 mM) were prepared in incomplete RPMI 1640 and mixed with parasite cultures (1% parasitemia and 1.5% hematocrit) in 96-well plates to a final drug concentration of 10 μM for hit identification studies, or 10–0.078 μM for activity confirmation assays. The final dimethyl sulfoxide (DMSO) concentration per 100 μL culture per well was 0.1%. Chloroquine and artemisinin at a range of 1–0.0078 μM each were used as negative growth control (positive test control), while the solvent-treated culture (0.1% DMSO) was used as positive growth control (negative test control). Following 72 h incubation at 37°C in a 5% CO_2 incubator, parasite growth was assessed by an SYBR green I-based DNA quantification assay. In brief, a 3x concentrated SYBR Green lysis buffer was added to each plate well containing parasitized erythrocytes and kept in the dark for about 30 minutes. Fluorescence was measured using a Fluoroskan Ascent multiwell plate reader with excitation and emission wavelengths at 485 and 538 nm, respectively. Mean half-maximal inhibitory concentrations (IC_{50} values) were derived by plotting percent growth against log drug concentration and fitting the response data to a variable slope sigmoidal curve function using GraphPad Prism v8.0.

2.5. Computational Methodology

2.5.1. Computational Tools. All *in silico* studies applied to this work were achieved using the following computational tool:

(a) ACDChemSketch® version 2.0, year 2020 used for modeling, first-hand, chemical structures to be fed for docking screening [12]

(b) Autodock Vina® tool version 1.2.0, year 2010 used for the virtual screening procedure [13]

(c) BIOVIA® Discovery Studio version 2021 used for the determination of binding pockets and for visualizing/analyzing the docked results [14]

(d) Absorption Distribution Metabolism Excretion and Toxicity of Structure Activity-Relationship (ADMETSAR): a web server used to evaluate the ADMET properties, biological activity, and drug-likeness [15–18]

2.5.2. Molecular Docking

(1) Ligand Preparations. In a quest to predict the antiplasmodial activity of the plant samples, compounds present in *Z. gilletii* were modeled using the ACDChem ChemSketch® version 2.0, year 2020 [12] computational tool and fed into Autodock vina® [13] for binding efficiency screening.

(2) Receptor preparations. The antiplasmodium receptor of PDB CODE, 5TBO, was used as the target receptor for this study. The receptor was obtained from the (RCSB) database (https://www.rcsb.org/pdb). The resolution of receptor 5TBO (2.15 Å) approximately lies about the 2.0 Å recommended resolution for a receptor of good quality [19]. Water molecules around the crystal structure and other associated inhibitors were removed from the downloaded protease to avoid undesired interferences and unwanted molecular interactions.

(3) Virtual screening. The virtual screening was done on *Z. gilletii* containing thirteen compounds using the Autodock vina® tool version 1.2.0, year 2010 [13] and Biovia Discovery Studio version 2021 [14]. The screening was guided using Chloroquine® and Artemether®, prominently used antiplasmodium therapeutics, as standards. Auto Dock Tools version 4.0 (ADT) was used to generate the autodock file (*.pdbqt* file) in preparation for docking. Other adjustments performed on both crystal structures include removing any extra water molecules, adding polar hydrogens, merging no-polar hydrogens, and adding Kollman charges. These adjustments are targeted at improving the affinity of the binding site. In modern computer-assisted drug design (CADD), the study of a potent drug is not complete without the activity study of the drug which is deducible from the compound's inhibition constant. A potent compound is expected to have inhibition constant values ranging between 0.01 and 1 μM for a potent drug; therefore, this parameter alone is enough to screen compounds in the drug discovery journey [19].

2.5.3. ADMET Studies. For predicting the toxicity level of the screened compounds, *in silico* toxicity studies were performed using the ADMETlab version 2.0 web server online [20]. Additionally, from the server, the absorption (human intestinal absorption), distribution (blood-brain barrier; water solubility), metabolism (cytochrome inhibition: CYP450), excretion (half-life), toxicity (hERG inhibition; carcinogenicity), and drug-likeness were computed. The results are summarized in Table 1.

3. Results and Discussion

3.1. Phytochemical Study. Thirteen compounds (Figure 1) have been isolated and characterized from the chemical investigation of the methanol extract of the bark of *Z. gilletii*. Based on their spectroscopic (^{1}H and ^{13}C) NMR and spectrometric (EI-MS) data (see Table 1S on

Table 1: ADMET score of qualified compounds from *Z. gilletii* with respect to the selected standards.

Compounds	HIA	BBB	Water solubility (mol/L)	CYP450 inhibition	hERG inhibition	Drug likeness (Lipinski)	$T_{(1/2)}$	Carcinogenicity
1	Yes (>60%)	No	Soluble (−3.615)	2/5	Inactive	Yes (5/5)	Short (0.255)	Yes
2	Yes (>90%)	No	Moderately soluble (−6.520)	3/5	Inactive	Yes (5/5)	Short (0.192)	Yes
3	Yes (>90%)	Yes	Soluble (−4.305)	4/5	Inactive	Yes (5/5)	Long 0.547	Yes
5	Yes (>90%)	No	Moderately soluble (−6.605)	3/5	Inactive	Yes (5/5)	Short 0.137	Yes
8	Yes (>90%)	Yes	Moderately soluble (−6.781)	1/5	Inactive	Yes (5/5)	Very short (0.041)	No
9	Yes (>90%)	No	Moderately soluble (−6.667)	0/5	Inactive	Yes (5/5)	Very short (0.037)	No
12	Yes (>90%)	No	Poorly soluble (−7.008)	1/5	Inactive	Yes (5/5)	Very short (0.030)	No
13	Yes (>60%)	No	Soluble (−4.793)	0/5	Inactive	Yes (5/5)	Very short (0.043)	No
Chloroquine	Yes (>90%)	Yes	Soluble (−3.902)	(2/5)	Inactive	Yes (5/5)	Very short (0.070)	No
Artemether	Yes (>90%)	No	Soluble (−4.677)	(0/5)	Inactive	Yes (5/5)	Very short (0.089)	No

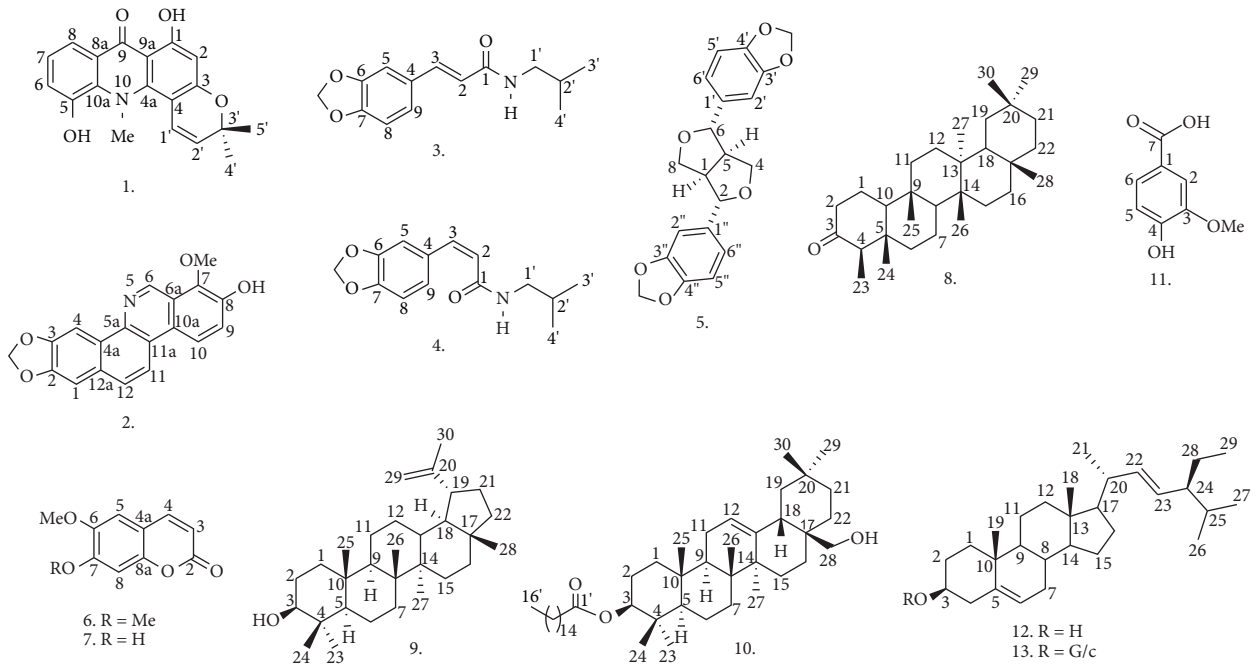

Figure 1: Chemical structures of compounds **1**–**13** isolated from *Z. gilletii*.

supplementary data), as well as the comparison of these data with those reported in the literature, the isolated compounds have been identified as 5-hydroxynoracronycine (**1**) [21], decarine (**2**) [22], *trans*-fagaramide (**3**) [23], *cis*-fagaramide (**4**) [24], sesamin (**5**) [25, 26], scoparone (**6**) [27], scopoletin (**7**) [28], fridelin (**8**) [29], lupeol (**9**) [30, 31], erythrodiol-3-*O*-palmitate (**10**) [32], vanillic acid (**11**) [23], stigmasterol (**12**), and stigmasterol-3-*O*-*β*-D-glucopyranoside (**13**) [31, 33].

3.2. In Vitro Antiplasmodial Activity. Among the isolated compounds, those in large amounts (compounds **1**, **3** + **4**, **5** and **9**) were submitted for *in vitro* antiplasmodial activity against the chloroquine-sensitive *P. falciparum* 3D7 (*Pf* 3D7) using chloroquine (IC_{50} = 24.74 nM) and artemisinin (IC_{50} = 17.76 nM) as reference drugs. All the compounds displayed good inhibition rates measured as **1** (54.69%), **3** + **4** (53.48%), **5** (51.89%), and **9** (52.64%). However, the most potent compound was the mixture **3** + **4** with an IC_{50}

value of 1333 nM while compounds **1**, **5**, and **9** were less or not active with IC_{50} values greater than 10,000 nM (Table 2). The inhibition level greater than 50% for all the compounds showed that the *Z. gilletii* extract is an important source of antiplasmodial compounds supporting the use of the plant in traditional medicine for the treatment of malaria and deserves further investigations in checking of synergistic effects of those compounds as well as the characterization of further constituents that can help in the development of new potent antimalarial drugs.

3.3. Molecular Docking. The binding affinities of all the thirteen compounds isolated from *Z. gilletii* as well as the selected standards (Chloroquine® and Artemether®) are given in Table 3 and Figure 2, while Figures 3–8 (also see Table 2S on supplementary data) show their binding interactions at the 5TBO receptor's binding site. The result shows that eight out of the thirteen identified compounds (**1**, **2**, **3**, **5**, **8**, **9**, **12**, **13**) were found to have a greater affinity to the antiplasmodium receptor than Artemether® while eleven compounds (**1**–**9**, **12**-**13**) were found to possess a greater affinity to the antiplasmodium receptor than Chloroquine®. This can also infer that the plant *Z. gilletii* has a high potency as an antiplasmodial agent. It can also be mentioned that since both standards used for this study (Chloroquine® and Artemether®) resulted in a maximum number of two conventional hydrogen bonds (Figure 8) while most selected compounds exhibited more, and with shorter bond length, it is understandable why the identified compounds have greater binding affinity to the antiplasmodium receptor than the standards.

3.4. ADMET Studies. The compounds displaying a good affinity (binding energy) to the 5TBO receptor binding site were further analysed for their ADMET properties, and the prediction results are presented in Table 1. The human intestinal absorption (HIA) of an oral drug is the essential prerequisite for its apparent efficacy. Furthermore, the close relationship between oral bioavailability and intestinal absorption has also been proven, and HIA can be seen as an alternative indicator for oral bioavailability to some extent. A drug molecule with an absorbance of less than 30% is poorly absorbed [20]. The results from Table 1 show that compounds **1**–**3**, **5**, **8**-**9**, **12**-**13** as well as both standard drugs (chloroquine and artemether) are strongly absorbed by the intestine.

Water solubility is one important condition that a drug must satisfy before the *in vitro* drug optimization process [20]. In this regard, the results show that all the identified compounds except compound **12** are water-soluble with −3.615, −4.305, and −4.793 for compounds **1**, **3**, and **13**, respectively, which are more soluble than the selected standards, chloroquine (−3.902) and artemether (−4.677).

Cytochrome P450 inhibitors are responsible for the biotransformation of a drug; a potential drug should not alter their kinetics [34]. The results show that although compounds **1** (2/5), **2** (3/5), **3** (4/5), and **5** (3/5) violated the minimum inhibition allowed as reported by Falade et al. [19], compounds **8** (0/5), **9** (0/5), **12** (1/5), and **13** (0/5) show an improved value of less inhibition compared to chloroquine (2/5).

Table 2: Antiplasmodial activity of compounds against *P. falciparum* 3D7.

Samples	% Inhibition[a]	IC_{50} (in nM)
1	54.69	>10,000
3 + **4**	53.48	1333
5	51.89	>10,000
9	52.64	>10,000
Chloroquine	61.86	24.74
Artemisinin	60.00	17.76

[a]Tested concentration: 10 μM.

Table 3: Binding energy of isolated compounds and standards to the anti-plasmodium (5TBO) receptor.

Compounds	Binding energy (ΔG) kcal/mol
1	−8.8
2	−9.5
3	−8.7
4	−7.3
5	−10.0
6	−7.3
7	−7.4
8	−8.3
9	−8.7
10	−7.1
11	−6.3
12	−8.6
13	−8.6
Chloroquine	−7.3
Artemether	−8.3

The human either-a-go-go related inhibition (hERG) is a measure of electrical pulse transmission in the human heart (iodine-channel blocking). A potential drug should not block the activity of the hERG inhibitors [34]. Table 1 shows that all compounds present themselves as inactive against blocking the heart functions, as the standards. Carcinogenicity results also show that compounds **8**, **9**, **12**, and **13** are noncarcinogenic to mammals. However, compounds **1**, **2**, **3**, and **5** are seen to be toxic.

Brain-blood barrier (BBB) prediction test suggests that compounds **1**, **2**, **5**, **9**, **12**, and **13** do not have the ability to cross the BBB; hence, their modes of action do not involve neurological engineering, such as appetite reduction as in chloroquine. It also suggests that the six (**6**) compounds will pose little or no side effects on administration as compared to chloroquine. However, compounds **3** and **8** have a tendency to cross the BBB.

A good drug must also be able to stay long (activity) enough in the body before excretion [35]. The half-life of a drug is the description of how long a drug will stay active in the body before excretion. Table 1 indicates that all identified compounds can exhibit a better excretion than the standard drugs.

In addition, Table 1 also describes the drug likeliness based on Lipinski's rules of five (5) criteria [36]. The rule

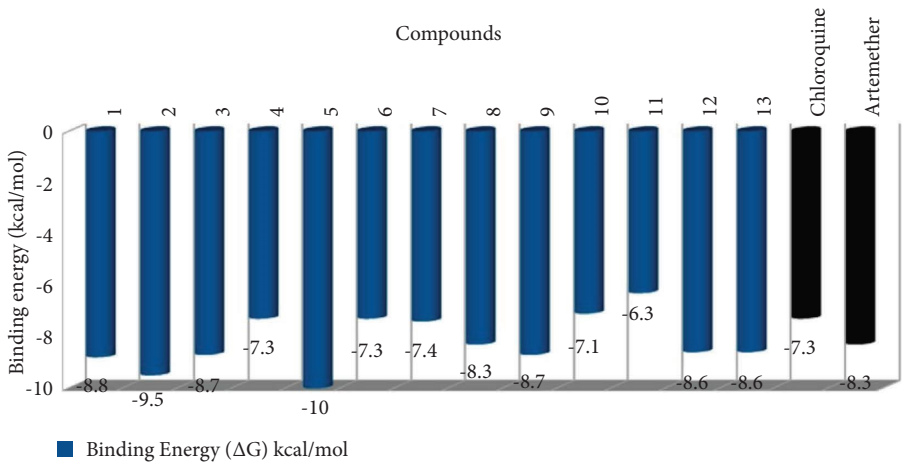

Figure 2: Graphical illustration of binding energy of the isolated compounds and standards to the anti-plasmodium (5TBO) receptor.

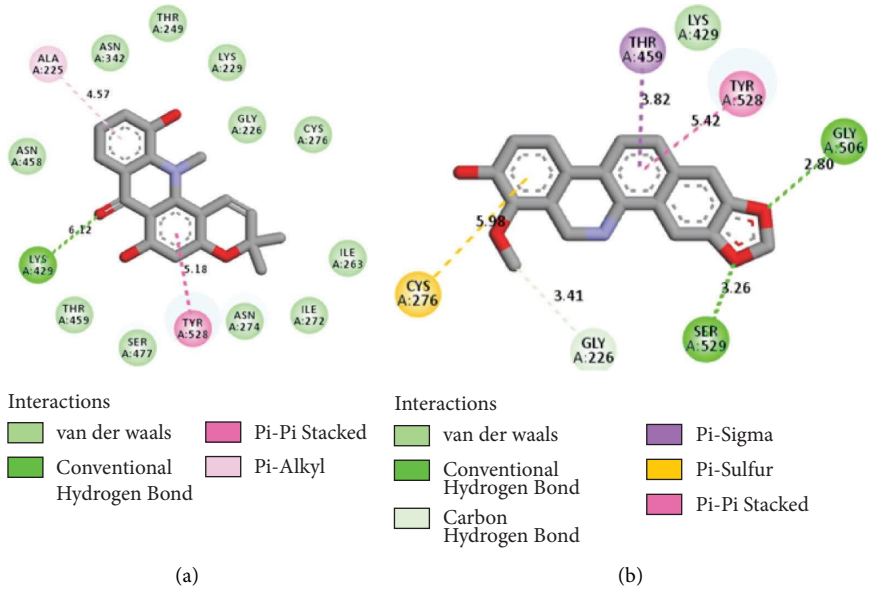

Figure 3: Docking poses of alkaloids **1** (a) and **2** (b) at the 5TBO receptor binding site.

states that for a compound that must stand as a potential drug, its structural properties must first satisfy the following rules: molecular weight ≤500; MiLOGP ≤4.15; number of oxygen ≤10; number of hydrogen ≤5; number of hydroxide ≤5.

Results show that all identified compounds satisfy this drug condition and hence are more likely to be applied as a drug.

3.5. Chemotaxonomic Significance. The purification of the *Z. gilletii* extract via successive column chromatography resulted in the isolation and identification of thirteen specialized metabolites including 5-hydroxynoracronycine (**1**), decarine (**2**), *trans*-fagaramide (**3**), *cis*-fagaramide (**4**), sesamin (**5**), scoparone (**6**), scopoletin (**7**), fridelin (**8**), lupeol (**9**), erythrodiol-3-O-palmitate (**10**), vanillic acid (**11**), stigmasterol (**12**), and its derivative stigmasterol-3-*O*-*β*-D-glucopyranoside (**13**).

Except compound **10** which is obtained here for the first time from the genus *Zanthoxylum* and in general from the family Rutaceae, all the other compounds have been previously reported from the genus *Zanthoxylum* or from the genus *Fagara* which contains several species which are synonyms of those classified in the genus *Zanthoxylum*. For instance, *trans*-fagaramide (**3**), scopoletin (**7**), and vanillic acid (**11**) have been previously reported from the bark of *Fagaramacrophylla* and *Fagara tessmannii* [23, 37]. These two species are both synonyms of *Z. gilletii*, the plant we have investigated. This result partially supports the taxonomy of our plant and its similarity with the two *Fagara* species based on their chemical constituents. Further evidence has been given by the identification of the other metabolites: the acridone alkaloids have been mainly isolated from the

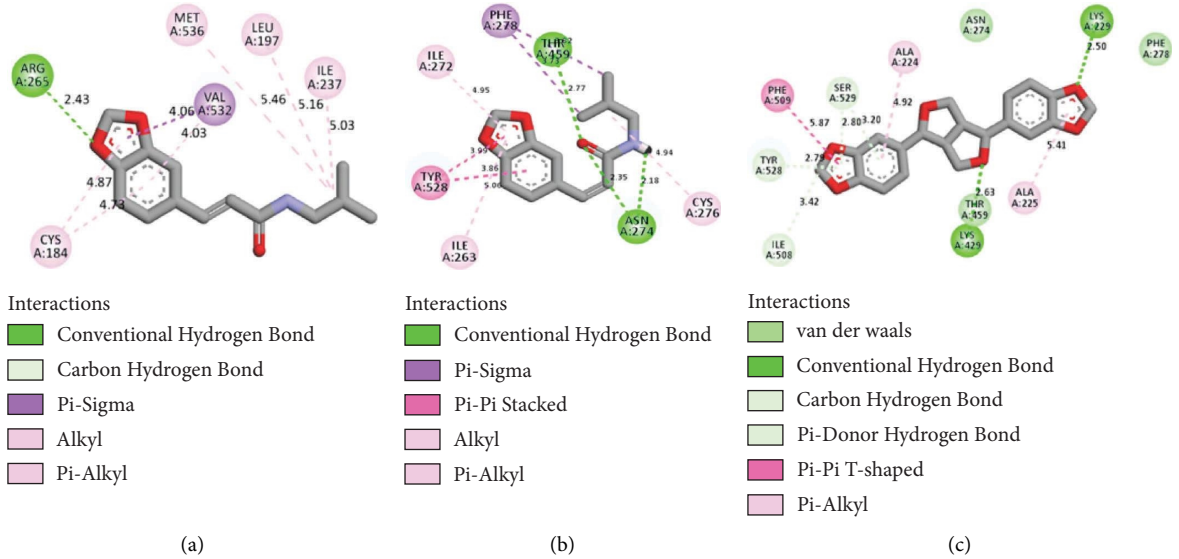

Figure 4: Docking poses of lignans **3** (a), **4** (b) and **5** (c) at the 5TBO receptor binding site.

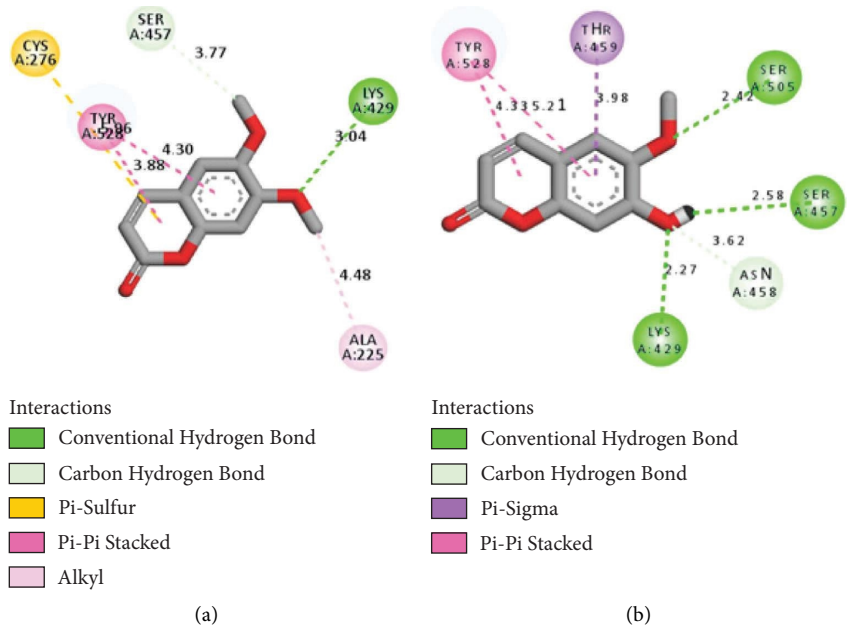

Figure 5: Docking poses of coumarins **6** (a) and **7** (b) at the 5TBO receptor binding site.

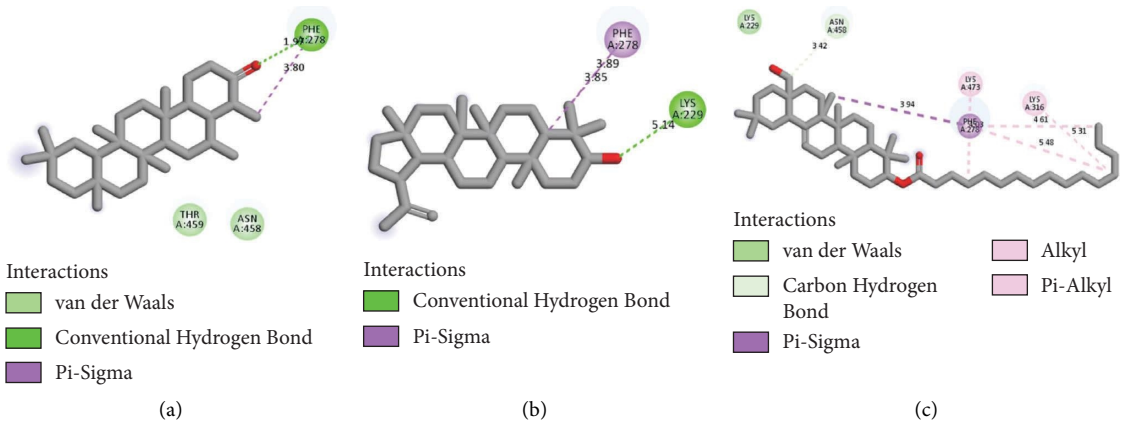

Figure 6: Docking poses of triterpenoids **8** (a), **9** (b) and **10** (c) at the 5TBO receptor binding site.

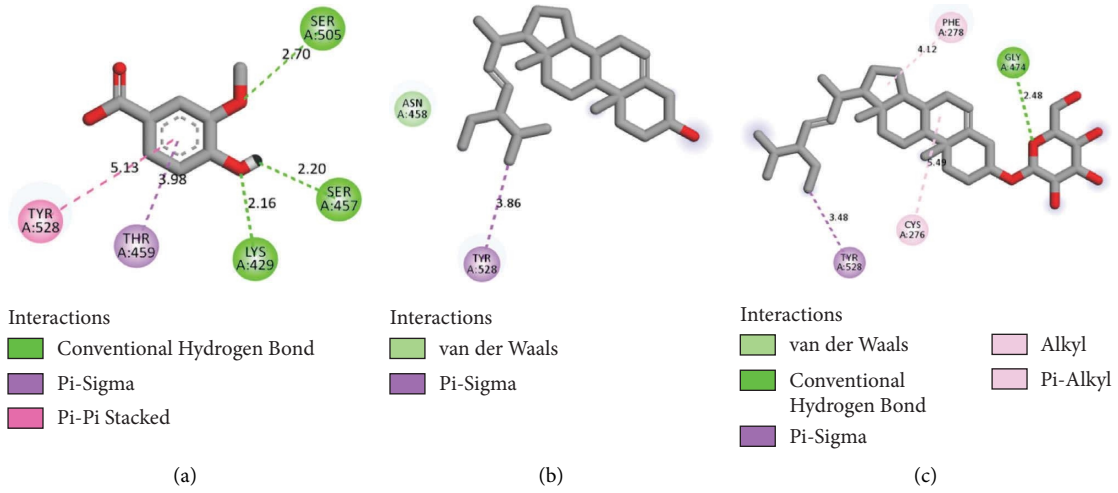

Figure 7: Docking poses of vanillic acid **11** (a), the steroids **12** (b) and **13** (c) at the 5TBO receptor binding site.

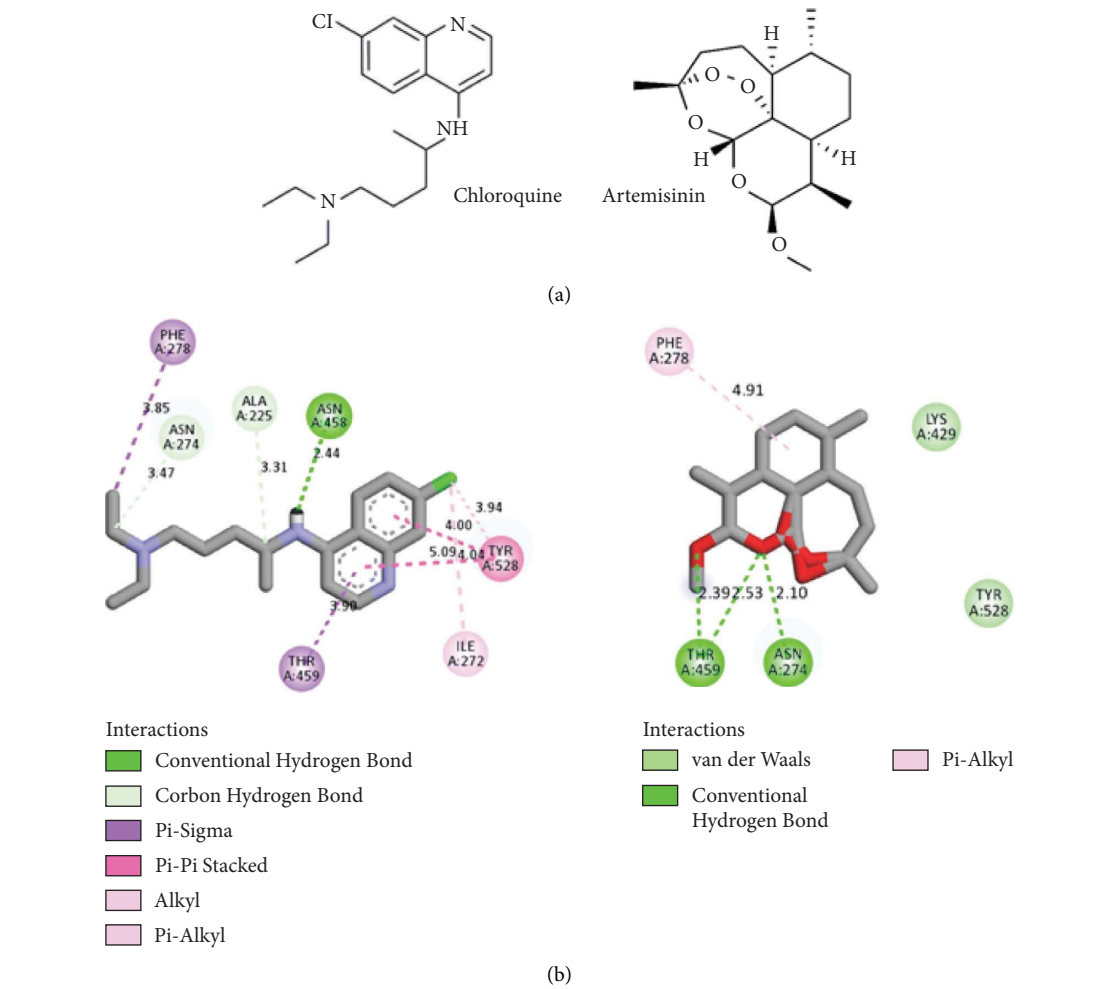

Figure 8: Structures of the standard drugs (a) and their docking poses (b) with the 5TBO receptor.

Rutaceae plants and more especially from the plants from the genus *Citrus*. Unsurprisingly, the acridone 5-hydroxynoracronycine (**1**) is one of the major compounds along with sesamin (**5**) which were already reported from the plant species *Z. poggei* and *Z. dinklagei* [21, 26], respectively, as well as for the first time to the best of our knowledge from *Z. gilletii*. Another lignan named *cis*-fagaramide (**4**) has been also isolated during our investigations but has been already identified by Cheng et al. in [16] during their works on *Z. schinifolium*. The alkaloid decarine (**2**) is obtained for the

first time from *Z. gilletii* while it has been found in *Z. madagascariense* [22]. Furthermore, the coumarin scopoletin (**6**) is widely encountered in many plant species and has been detected and characterized from the species *Z. rhetsa*, *Z. schinifolium*, and *Z. leprieurii* [27, 38, 39]. The two triterpenoids fridelin (**8**) and lupeol (**9**) are also mainly distributed in several plants and within the family Rutaceae, and they have been isolated from *Z. schinofolium*, *Z. tessmannii*, or *Citrus aurantium* [24, 29, 40]. However, the third triterpene identified as erythrodiol-3-O-palmitate (**10**) has not been previously obtained from the family Rutaceae as indicated earlier. Compound **10** is a derivative of β-amyrin belonging to the oleanane-type triterpenoids [41]. The literature survey indicates that some congeners of compound **10** including β-amyrin or β-amyrin acetate have already been reported from the *Zanthoxylum* genus. Indeed, β-amyrin was obtained in *Z. simulans* and *Z. nitidum* [42, 43], while β-amyrin acetate was reported from the species *Z. schinifolium* [24]. This evidence strongly supported the possibility of obtention of erythrodiol-3-O-palmitate (**10**) which is very structurally close to β-amyrin acetate and differs from it by just the length of the fatty acid attached to C-3 as well as the oxidation of the methyl CH_3-28 to a primary alcohol function CH_2OH [41]. Erythrodiol-3-O-palmitate (**10**) has been previously obtained from *Trilepsium madagascariense* (Moraceae) [32] and is reported for the first time from *Z. gilletii* and the family Rutaceae. Finally, the steroids stigmasterol (**12**) and stigmasterol-3-O-β-D-glucopyranoside (**13**) are usually obtained from several plant materials. Thus, all the chemical compounds isolated from *Z. gilletii* provide clear insights supporting the taxonomy of the plant and enrich the knowledge of its chemistry.

4. Concluding Remarks

Thirteen compounds (**1**–**13**) have been isolated and characterized from the phytochemical investigations of the methanol extract of the bark from *Z. gilletii*, a Cameroonian medicinal plant. The compounds have been sorted into six main classes of compounds including two alkaloids (**1** and **2**), three lignans (**3**–**5**), two coumarins (**6** and **7**), three pentacyclic triterpenoids (**8**–**10**), one phenolic compound (**11**) as well as two steroids (**12** and **13**). The chemotaxonomic significance of the isolated compounds strengthened the classification of the plant in the Rutaceae family and provided additional compounds to enrich the chemistry of the species *Z. gilletii* (Rutaceae). More interestingly, all the compounds tested *in vitro* showed good inhibition rates of *Pf* 3D7 with values greater than 50% while the molecular docking of the isolated compounds showed that a total of eleven compounds displayed a good affinity with the 5TBO receptor binding site compared to the standard drugs chloroquine and artemether. Likewise, the ADMET study indicated that isolated compounds exhibited good and favourable parameters that qualify them as good candidates for drug development. The present study, in addition to supporting the use of the plant in traditional medicine for the treatment of malaria, gives significant insights for further *in vitro* and *in vivo* pharmacological investigations in the discovery of new antimalarial drugs.

Data Availability

The spectroscopic (^{1}H and ^{13}C-NMR) and spectrometric (EI-MS) data (Table 1S) of all the isolated compounds and their molecular docking data (Table 2S) used to support the findings of this study are included within the supplementary information file.

Conflicts of Interest

The authors declare that they have no conflicts of interest.

Supplementary Materials

Table 1S shows the mass and NMR data of isolated compounds. Table 2S shows compounds from *Z. gilletii* and their interactions at the 5TBO receptor binding site. (*Supplementary Materials*)

References

[1] G. M. Happi, L. Z. Meikeu, K. G. Sikam, L. C. Dzouemo, and J. D. Wansi, "Mushrooms (Basidiomycetes) as a significant source of biologically active compounds for malaria control," *Natural Resources for Human Health*, vol. 2, no. 2, pp. 129–141, 2022.

[2] Who, *World Malaria Report 2019*World Health Organization, Geneva, Switzerland, 2019.

[3] Severe Malaria Observatory, *Le paludisme au Cameroun*, World Health Organization, Geneva, Switzerland, 2020.

[4] G. M. Happi, S. F. Kouam, F. M. Talontsi et al., "Antiplasmodial and cytotoxic triterpenoids from the bark of the Cameroonian medicinal plant Entandrophragma congoënse," *Journal of Natural Products*, vol. 78, no. 4, pp. 604–614, 2015.

[5] M. J. O'Neill, D. H. Bray, P. Boardman et al., "Plants as sources of antimalarial drugs, Part 4: activity of Brucea javanica fruits against chloroquine-resistant Plasmodium falciparum in vitro and against Plasmodium berghei in vivo," *Journal of Natural Products*, vol. 50, no. 1, pp. 41–48, 1987.

[6] G. Gaya, J. F. Kawaka, A. Muchugi, and J. J. Ngeranwa, "Variation of alkaloids in the Kenyan Zanthoxylum gilletii (de wild waterman)," *African Journal of Plant Science*, vol. 7, no. 9, pp. 438–444, 2013.

[7] C. Orwa, A. Mutua, R. Kindt, R. Jamnadass, and A. Simons, *Agroforestree Database: a tree reference and selection guide*, World Agroforestry Centre, Nairobi Kenya, 2009.

[8] G. Zirihi, K. N'guessan, D. Etien, and B. Serikouassi, "Evaluation in vitro of antiplasmodial activity of ethanolic extracts of Funtumia elastica, Rauvolfia vomitoria and Zanthoxylum gilletii on Plasmodium falciparum isolates from Côte d'Ivoire," *Journal of Animal and Plant Sciences*, vol. 5, pp. 406–413, 2009.

[9] G. N. Zirihi, D. J. Yao, K. M. Kra-Adou, and P. Grellier, "Phytochemical and pharmacological studies of alcoholic extract of Fagara macrophylla (Oliv) Engl (Rutaceae): chemical structure of active compound inducing antipaludic activity," *Journal of Chinese Clinical Medecine*, vol. 2, pp. 205–210, 2007.

[10] G. M. Happi, P. K. Nangmo, L. C. Dzouemo, S. F. Kache, A. D. K. Kouam, and J. D. Wansi, "Contribution of Meliaceous plants in furnishing lead compounds for antiplasmodial and insecticidal drug development," *Journal of Ethnopharmacology*, vol. 285, Article ID 114906, 2022.

[11] K. P. Yemback, E. K. Oben, N. M. Efange et al., "Glyceraldehyde-3-phosphate dehydrogenase (PfGAPDH): Design, isolation, synthesis and preliminary anti-malarial activity against Plasmodium falciparum 3D7 strains," *Research Square*, pp. 1–15, 2022.

[12] A. C. D. ChemSketch, *Advanced Chemistry Development Inc*ACD labs, Toronto, ON, Canada, 2020.

[13] O. Trott and A. J. Olson, "Software news and update AutoDockVina: improving the speed and accuracy of docking with a new scoring function, efficient optimization, and multithreading," *Journal of Computational Chemistry*, vol. 31, pp. 455–461, 2010.

[14] D. Biovia, "BIOVIA workbook," *BIOVIA Pipeline Pilot*, Dassault Systèmes, San Diego, 2021.

[15] K. Tsaioun and S. A. Kates, *ADMET for Medicinal Chemists: A Practical Guide*, John Wiley & Sons, Singapore, 2010.

[16] F. Cheng, W. Li, Y. Zhou et al., "admetSAR: a comprehensive source and free tool for assessment of chemical ADMET properties," *Journal of Chemical Information and Modeling*, vol. 52, no. 11, pp. 3099–3105, 2012.

[17] A. Daina, O. Michielin, and V. Zoete, "SwissADME: a free web tool to evaluate pharmacokinetics, drug-likeness and medicinal chemistry friendliness of small molecules," *Scientific Reports*, vol. 7, no. 1, Article ID 42717, 2017.

[18] H. Yang, C. Lou, L. Sun et al., "admetSAR 2.0: web-service for prediction and optimization of chemical ADMET properties," *Bioinformatics*, vol. 35, no. 6, pp. 1067–1069, 2018.

[19] V. A. Falade, T. I. Adelusi, I. O. Adedotun, M. Abdul-Hammed, T. A. Lawal, and S. A. Agboluaje, "In silico investigation of saponins and tannins as potential inhibitors of SARS-CoV-2 main protease (Mpro)," *In Silico Pharmacology*, vol. 9, no. 1, pp. 9–15, 2021.

[20] G. Xiong, Z. Wu, J. Yi et al., "ADMETlab 2.0: an integrated online platform for accurate and comprehensive predictions of ADMET properties," *Nucleic Acids Research*, vol. 49, no. 1, pp. W5–W14, 2021.

[21] J. D. Wansi, A. Tadjong Tcho, F. A. A. Toze, L. Nahar, C. Martin, and S. D. Sarker, "Cytotoxic acridone and indoloquinazoline alkaloids from Zanthoxylum poggei," *Phytochemistry Letters*, vol. 17, pp. 293–298, 2016.

[22] M. T. Martin, L. H. Rasoanaivo, and A. Raharisololalao, "Phenathridine alkaloids from Zanthoxylum madagascariense," *Fitoterapia*, vol. 76, no. 6, pp. 590–593, 2005.

[23] J. D. Wansi, S. O. Nwozo, L. M. Mbaze et al., "Amides from the stem bark of Fagara macrophylla," *Planta Medica*, vol. 75, no. 05, pp. 517–521, 2009.

[24] M.-J. Cheng, C.-H. Yang, W.-Y. Lin, W.-Y. Lin, I.-L. Tsai, and I.-S. Chen, "Chemical constituents from the leaves of Zanthoxylum schinifolium," *Journal of the Chinese Chemical Society*, vol. 49, no. 1, pp. 125–128, 2002.

[25] F. Fish, P. G. Waterman, and N. Finkelstein, "Sesamin from the bark of two African Zanthoxylum species," *Phytochemistry*, vol. 12, no. 10, pp. 2553-2554, 1973.

[26] F. Fish, I. A. Meshal, and P. G. Waterman, "Alkaloids, triterpenes, and lignans from the bark of Zanthoxylum dinklagei," *Phytochemistry*, vol. 14, no. 9, p. 2094, 1975.

[27] G. B. Tabekoueng, C. Mvot Akak, M. K. Langat et al., "Chemical constituents from Penianthus camerounensis dekker (menispermaceae)," *Zeitschrift für Naturforschung B*, vol. 74, no. 10, pp. 703–708, 2019.

[28] G. M. Happi, G. P. Mouthe Kemayou, H.-G. Stammler et al., "Three phragmalin-type limonoids orthoesters and the structure of odoratone isolated from the bark of *Entandrophragma candollei* (Meliaceae)," *Phytochemistry*, vol. 181, Article ID 112537, 2021.

[29] S. M. Bissim, S. B. Kenmogne, A. T. Tcho et al., "Bioactive acridone alkaloids and their derivatives from *Citrus aurantium* (Rutaceae)," *Phytochemistry Letters*, vol. 29, pp. 148–153, 2019.

[30] L. V. L. Bongmo, A. B. Nouga, G. M. Happi et al., "Phytochemical compounds of Guibourtia ehie and their antioxidant, urease and α-glucosidase inhibitory activities," *Natural Resources for Human Health*, vol. 2, no. 3, pp. 306–312, 2022.

[31] L. D. F. Tsamo, L. V. Yimgang, S. C. N. Wouamba et al., "A new ceramide (rumexamide) and other chemical constituents from *Rumex abyssinicus* jacq (polygonaceae): isolation, characterization, antibacterial activities and chemophenetic significance," *Advances in Biological Chemistry*, vol. 11, no. 05, pp. 266–282, 2021.

[32] P. Y. Ango, D. W. F. G. Kapche, V. Kuete, B. T. Ngadjui, M. Bezabih, and B. M. Abegaz, "Chemical constituents of *Trilepisium madagascariense* (Moraceae) and their antimicrobial activity," *Phytochemistry Letters*, vol. 5, no. 3, pp. 524–528, 2012.

[33] W. D. T. Tsopgni, G. M. Happi, H.-G. Stammler et al., "Chemical constituents from the bark of the Cameroonian mahogany *Trichilia emetica* Vahl (Meliaceae)," *Phytochemistry Letters*, vol. 33, pp. 49–54, 2019.

[34] M. C. Sanguinetti and M. Tristani-Firouzi, "hERG potassium channels and cardiac arrhythmia," *Nature*, vol. 440, no. 7083, pp. 463–469, 2006.

[35] C. A. Lipinski, F. Lombardo, B. W. Dominy, and P. J. Feeney, "Experimental and computational approaches to estimate solubility and permeability in drug discovery and development settings," *Advanced Drug Delivery Reviews*, vol. 64, pp. 4–17, 2012.

[36] C. A. Lipinski, "Avoiding investment in doomed drugs," *Journal of Current Drug Discovery*, vol. 1, pp. 17–19, 2001.

[37] L. M. Mbaze, H. M. P. Poumale, J. D. Wansi et al., "α-Glucosidase inhibitory pentacyclic triterpenes from the stem bark of Fagara tessmannii (Rutaceae)," *Phytochemistry*, vol. 68, no. 5, pp. 591–595, 2007.

[38] A. T. Tchinda, V. Feundjiep, A. Sajjad et al., "Bioactive compounds from the fruits of Zanthoxylum leprieurii," *Pharmacologyonline*, vol. 1, pp. 406–415, 2009.

[39] W. Li, W. Zhou, S. H. Shim, and Y. H. Kim, "Chemical constituents of Zanthoxylum schinifolium (Rutaceae)," *Biochemical Systematics and Ecology*, vol. 55, pp. 60–65, 2014.

[40] C. Kenmoe Djeukeu, A. Kouam Kenmogne, A. Guy Blaise Azebaze et al., "A new aromatic amide from the roots of *Zanthoxylum tessmannii* (Rutaceae)," *Chemistry and Biodiversity*, vol. 16, no. 4, Article ID e1800590, 2019.

[41] G. M. Happi, V. K. Ntabo, A. T. Tcho, and J. D. Wansi, "Naturally occurring dimeric triterpenoids: o," *Phytochemistry*, vol. 200, Article ID 113242, 2022.

[42] K. Deyun, A. I. Gray, T. G. Hartley, and P. G. Waterman, "Alkaloids from an Australian accession of Zanthoxylum nitidum (Rutaceae)," *Biochemical Systematics and Ecology*, vol. 24, no. 1, pp. 87-88, 1996.

[43] I.-S. Chen, I.-W. Tsai, C.-M. Teng et al., "Pyranoquinoline alkaloids from Zanthoxylum simulans," *Phytochemistry*, vol. 46, no. 3, pp. 525–529, 1997.